Research Journal of Applied Sciences, Engineering and Technology 5(1): 203-208, 2013
DOI:10.19026/rjaset.5.5105
ISSN: 2040-7459; e-ISSN: 2040-7467

Submitted: May 16, 2012 Accepted: June 15, 2012 Published: January 01, 2013

Research Article

Concept of Recombination Velocity S_{fcc} at the Junction of a Bifacial Silicon Solar Cell, in Steady State, Initiating the Short-Circuit Condition

[1]I.ly, [2]M. Ndiaye, [1]M. Wade, [2]Ndeye Thiam, [2]Sega Gueye and [2]G. Sissoko
[1]Ecole Polytechnique of Thies, EPT, Thies, Senegal
[2]Faculty of Science and Technology, University Cheikh Anta Diop, Dakar, Senegal

Abstract: The aim of this study is to present technics to determine the junction recombination velocity of a bifacial polycrystalline silicon solar cell under both, constant multispectral illumination and steady short-circuit condition.

Keywords: Bifacial silicon solar cell, junction recombination velocity, short-circuit

INTRODUCTION

Our contribution consists in proposing technics that determine the junction recombination velocity S_{fcc} of a bifacial polycrystalline silicon solar cell in steady state and under constant multispectral light, initiating the short-circuit condition. Thus, we basically present a theoretical survey, in which we schematize an isolated grain of the solar cell (Blakers *et al*., 1989; Huljié *et al*., 2001).

As the shunt resistance R_{sh} is expressed as a calibrated function of S_f while the solar cell is under short-circuit, represented by S_{fcc}, the determination of Sfcc lead to the exact value of Rsh (Mbodji *et al*., 2010). In solving the continuity equation, we define the expressions of the charge carriers' density (Endrös and Martinelli, 1997) and deduce the photocurrents that let us introduce the concept of the recombination velocities at the junction yielding the short-circuit photocurrent density (Mbodji *et al*., 2012). Then we will discuss the results that we have obtained before we make a conclusion.

Theory: On behalf of the study, the solar cell placed under different levels of light is illuminated on its front, back and then simultaneously on its two sides. The model is treated as one dimensional with the origin of the solar cell junction.

During the direct conversion of the radiation energy into electric energy, two important phenomena influence the solar cell's efficiency.

These are absorption of the light (photons) by the cell and generation of electron hole pairs. These absorption and generation phenomena are of a paramount importance in determining the solar cell's electronic and electric parameters and are governed by the equation of continuity (1), and this equation lets determine the minority carriers' density of the photo-generated charges according to the illumination mode.

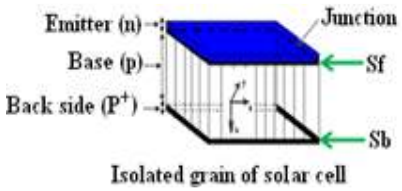

Fig. 1: Polycrystalline solar cell's structure

In these conditions and in steady state, the equation of continuity for a one-dimensional study to which obey these charge minority carriers in the base of the x-axis is announced as follows (Fig. 1):

$$\frac{\partial^2 \delta_\alpha(x)}{\delta x^2} - \frac{\delta_\alpha(x)}{L^2} = -\frac{1}{D} G_\alpha(x) \quad (1)$$

δ_α (x) is the excess minority carriers density according to the depth x in the base following the different illumination modes; α symbolizes the illumination mode with:

α = 1, α = 2, α = 3 for a respective light of the front side, back side and simultaneously both sides of the solar cell.

L and D are respectively the excess minority carrier's diffusion length and coefficient in the base.

G_α (x) is the generation rate of the excess minority carriers to an x distance in the base of the solar cell.

The expression of G^α (x) depends on the x depth of light absorption in the base and can be written in the form of the following equation:

$$G_\alpha(x) = n\sum_{i=1}^{3} a_i \begin{bmatrix} \xi_\alpha e^{-b_i x} \\ + \chi_\alpha e^{-b_i (H-x)} \end{bmatrix} \quad (2)$$

Corresponding Author: G. Sissoko, Faculty of Science and Technology, University Cheikh Anta Diop, Dakar, Senegal

Table1: The illumination mode parameters

Illumination mode	ξ_α	χ_α
Front side illumination α = 1	1	0
Back side illumination α = 2	0	
Both sides simultaneous illumination α = 3	1	1

H = thickness of the base;

The parameters a_i and b_i stem from the modeling of the incident illumination as defined by (Mohammad, 1987) under A.M 1.5 condition.

where, $a_1 = 6.13\text{x}10^{20}$ cm^{-3}/s; $a_2 = 0.54\text{x}10^{20}$ cm^{-3}/s; $a_3 = 0.0991\text{x}10^{20}$ cm^{-3}/s; $b_1 = 6630$ cm^{-1}; $b_2 = 103$ cm^{-1}; $b_3 = 130$ cm^{-1}; n = the number of sun linking the real incident power to the reference power for a given solar spectrum. It is defined as follows:

$$n = \frac{I_{cci}}{I_{cco}} \tag{3}$$

With, I_{cci} the short-circuit photocurrent density obtained from a solar cell under A.M 1.5 condition and I_{cco} is the short-circuit current reference measured for given illumination light. The coefficients ξ_α and χ_α are defined following the solar cell's illumination modes. They are given in Table 1:

The solution $\delta_\alpha(x)$ of the carriers' diffusion Eq. (1) can be made in the following forms:

$$\delta_\alpha(x) = A_\alpha.ch\left(\frac{x}{L}\right) + B_\alpha.sh\left(\frac{x}{L}\right) - \sum_{i=1}^{3} K_i.(\xi_\alpha e^{-b_i.x} + \chi_\alpha e^{-b_i.(H-x)}) \tag{4}$$

The coefficients A_α and B_α (α = 1, 2, 3) can be determined from the boundary conditions at the junction and at the back side (Bowden and Rohatgi, 2001; Möller, 1993; Alain, 1997) defined as follows:

At the junction emitter-base (for x = 0):

$$\frac{\partial\delta_\alpha(x)}{\partial x}\Big|_{x=0} = \frac{S_{f\alpha}}{D}.\delta_\alpha(0) \tag{5}$$

At the back side of the base (for x = H):

$$\frac{\partial\delta_\alpha(x)}{\partial x}\Big|_{x=H} = -\frac{S_{b\alpha}}{D}.\delta_\alpha(H) \tag{6}$$

$S_{f\alpha}$ and $S_{b\alpha}$ represent respectively the recombination velocities of the excess minority carriers

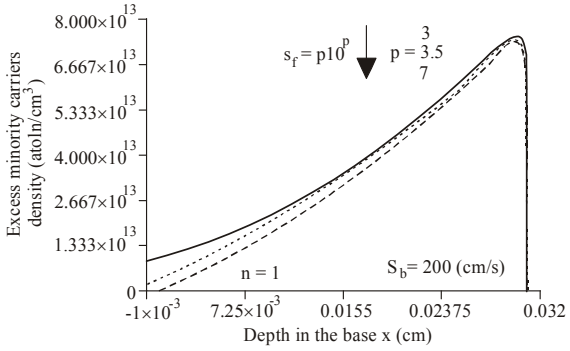

Fig. 2: Carriers' density according to the x depth in the base for a front side illumination ($S_f = px10^p$ cm/s, $S_b = 200$ cm/s, D = 26 cm^2/s, L = 0.015 cm and n = 1)

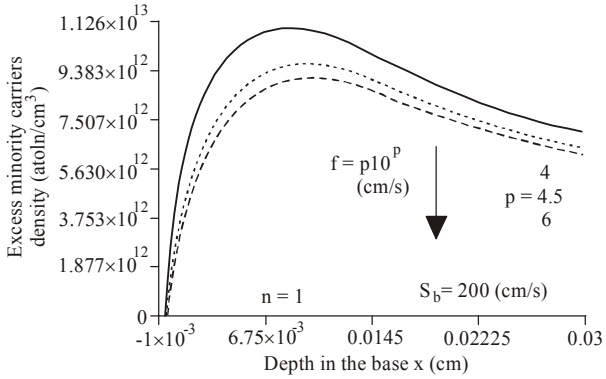

Fig. 3: Carriers' density according to the x depth in the base for a back side illumination ($S_f = px10^p$ cm/s with S_b = 200 cm/s, D = 26 cm^2/s, L = 0.015 cm and n = 1)

at the junction and at the back side (Diallo *et al*., 2008). And K_i is defined as follows:

$$K_i = \frac{nL^2.a_i}{D(b_i^2.L^2 - 1)} \tag{7}$$

With:

$$D(b_i^2.L^2 - 1) \neq 0 \tag{8}$$

By introducing the coefficients A_α and B_α respectively in the Eq. (4), we obtain the different expressions of the excess minority carriers density.

And in pointing up the effect of the high recombination velocities to the junction, the profiles of the minority carriers' density in excess depending on the x depth in the base and according to the different illumination modes are represented in the following Fig. 2, 3 and 4.

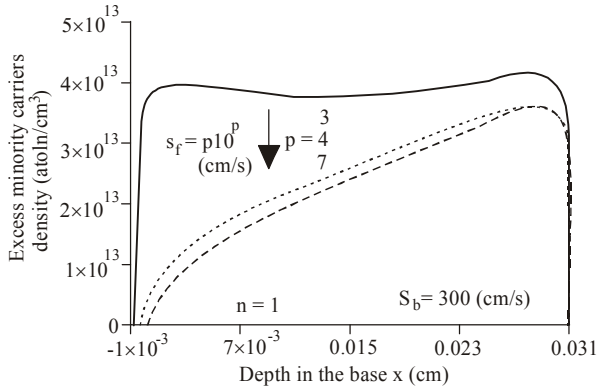

Fig. 4: Carriers' density according to the x depth in the base for both sides simultaneous illumination (S_b = 3x10^3 cm/s, D = 26 cm^2/s, L = 0.015 cm and n = 1)

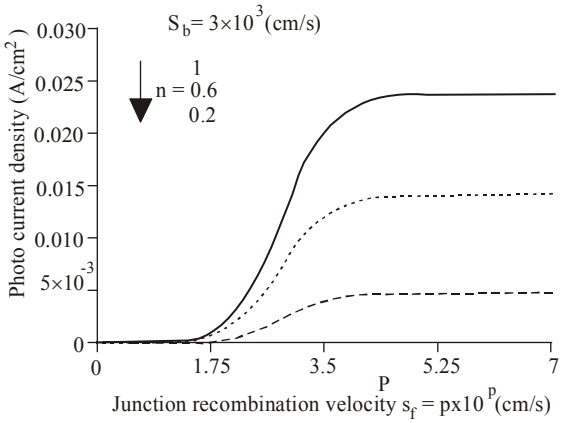

Fig. 5: Current density versus Log (S_f) for front side illumination and n illumination level (S_{b1} = 3x10^3 cm/s, D = 26 cm^2/s, L = 0.015 cm and H = 0.03 cm)

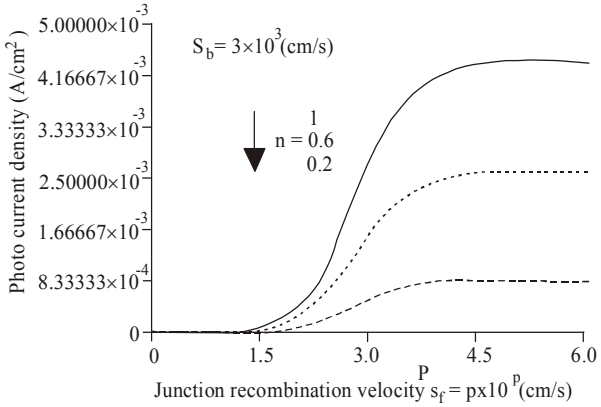

Fig. 6: Current density versus Log (S_f) for back side illumination and n illumination level (S_{b1}=3x10^3 cm/s, D = 26 cm^2/s, L = 0.015 cm for three level of n)

According to the Eq. (5) which governs the boundary's conditions at the junction, the excess minority carriers density δ_α (x) is intimately linked at the recombination velocity of the excess minority carriers at the junction S_f and depth in the base. We have different characteristical regions when the solar cell is illuminated differently.

In Fig. 2, when the solar cell is illuminated in front side, the excess minority carriers density δ_1 (x) increase and achieve a maxima point near the junction and decrease to minimum in the back side of the solar cell. When the solar cell is illuminated in rear side (Fig. 2), δ_2 (x) increase from junction to a maxima point situated in the back side of the solar cell. We note that in Fig. 3, for the low values of junction recombination velocity S_f, the first maxima point is near the junction but for the high values of S_f, the second maxima point is at the rear side of the solar cell.

Concept of the recombination velocity to the junction initiating the short-circuit: From the expressions of the excess minority carriers density, in this part of the study, the survey deals with photocurrent densities profiles according to the recombination velocity to the junction among other parameters. These profiles are drawn on behalf of the three illuminations modes. From these profiles, we will study technics to determine the recombination velocity to the junction initiating the short circuit, its validity domain as well. And in a way these velocities expressed with a p parameter are put in the form of the following Eq. (9):

$$S_{f\alpha}(p) = p \cdot 10^{p} \quad (9)$$

Photocurrent density survey for the different light modes: The expression of the photocurrent density is obtained from the following relation:

$$J_{ph_\alpha} = q.D.\frac{\partial \delta_\alpha(x)}{\partial x}\Big|_{x=0} \quad (10)$$

where, q = 1.6x1019 C is the charge of the electron.

The expression (10) of the current density and on behalf of the three illumination modes (α = 1 or 2 or 3) lets us draw its variation according to the recombination velocity at the junction and for different values of the illumination level.

We plot in Fig. 5, 6 and 7 photocurrent density versus Log (S_f) respectively for front side, back side and simultaneous n illumination level.

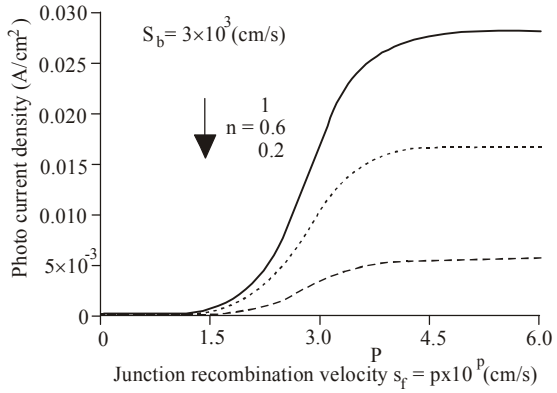

Fig. 7: Current density versus Log (S_f) for simultaneous illumination and n illumination level (S_{b1} = 3×10^3 cm/s, D = 26 cm^2/s, L = 0.015 cm and H = 0.03 cm, for three level of n)

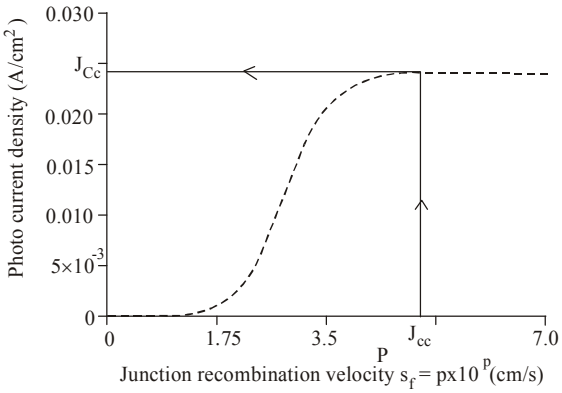

Fig. 8: Technics to determine the short-circuit current

The curves present two stages for all three figures: We note that the photocurrent's density increases with the recombination velocity up to a value where it remains constant whatever the illuminations mode and level. This constant value of photocurrent is called the short-circuit photocurrent. It depends on illumination mode and occurs when the junction recombination velocity is greater than 4×10^4 cm/s as shown in Diallo *et al*. (2008).

For the low values of S_f which are smallest than $1.5\times10^{1.5}$ cm/s, the photocurrent density is near zero.

Recombination velocity to the junction $S_{fcc\alpha}$ for different modes and levels of the solar cell's light: The condition of short-circuit is a situation of total shift to the emitter of all the electrons photo-generated in the base and that cross the junction. And according to the currents' profile below, this situation of short-circuit appears to the high values of the recombination velocity to the junction $S_{f\alpha}$. For such a situation, there is not any longer some carriers to the junction storing and the photocurrent is maximal and tends asymptotically to a constant value.

This fact is mathematically due to the following equation:

$$\frac{\partial J_{ph\alpha}}{\partial S_{f\alpha}} = 0 \tag{11}$$

In other terms, the general expression of the short-circuit's current's density is (Ba *et al*., 2003):

$$J_{cc\alpha} = \lim_{S_{f\alpha}\to\infty} J_{ph\alpha} \tag{12}$$

The first intercept point between the calibrated function $J_{ph\alpha}(S_{f\alpha})$ and the short circuit current $J_{cc\alpha}$ yields the value of the recombination velocity to the junction. So, this will be deduced from the following equation for the three illumination modes:

$$J_{ph\alpha}(S_{f\alpha}) - J_{cc\alpha} = 0 \tag{13}$$

Technics to determine short-circuit current: The Fig. 8 elucidates this technics that lets determine the short-circuit current for a recombination velocity to the given junction. We focus on a particular velocity of recombination to the junction. It's the one that initiates the short-circuit current and in the example that we have given, it is equal to $S_{fcc} = 4.9x10^{4,9}$ cm/s. The projection of the line $X = p = 4.9x10^{4,9}$ on the current variation curve J_{ph} (n, p, m) according to the recombination velocity S_f we give an intersection point. The projection of this intersection point Y-axis dives us the precise value of the short-circuit current.

However, this technics to determine the short-circuit current has some limits. Particularly, for some recombination velocities to the junction inferior to the ones initiating the short-circuit current, this technics is not usable. Its validity domain is defined for recombination velocities superior or equal to a reference velocity and in our case $4.9x10^{49}$ cm/s.

Recombination velocity to the junction: In resolving the Eq. (13) that becomes (14), we can deduce from there the recombination velocity at the junction for the three illumination modes.

Table 2: Recombination velocity to the junction S_{fcc1} initiating the short-circuit current for solar cell's front side illuminated

Light level (n)	1	0.6	0.2
Short circuit current J_{cc1} (A)	$23.53.10^{-3}$	$14.11.10^{-3}$	$4.67.10^{-3}$
Velocity S_{b1}(cm / s)	3.10^{3}	3.10^{3}	3.10^{3}
S_{fcc1} (cm / s) initiating the short circuit current $_{cc1}$(A)	$3.89.10^{6}$	$2.09.10^{6}$	$5.46.10^{5}$

Table 3: Recombination velocity to the junction S_{fcc2} initiating the short-circuit current for a back side illumination

Light level (n)	1	0.6	0.2
Short circuit current J_{cc2} (A)	$4.30.10^{-3}$	$2.57.10^{-3}$	$8.55.10^{-4}$
Velocity S_{b2}(cm/s)	3.10^{3}	3.10^{3}	3.10^{3}
S_{fcc2} (cm/s) initiating the short circuit current J_{cc2}(A)	$2.30.10^{5}$	$1.52.10^{5}$	$1.33.10^{5}$

Table 4: The recombination velocity to the junction S_{fcc3} initiating the short-circuit current for a simultaneous light

Light level (n)	1	0.6	0.2
Short circuit current J_{cc3} (A)	$27.96.10^{-3}$	$16.77.10^{-3}$	$5.58.10^{-3}$
Velocity S_{b3} (cm/s)	3.10^{3}	3.10^{3}	3.10^{3}
S_{fcc3} (cm/s) initiating the short circuit current J_{cc3}(A)	$4.23.10^{6}$	$2.26.10^{6}$	$6.76.10^{5}$

$$J_{ph\alpha}(S_f)-J_{c\alpha}=q.S_f .\left(\frac{B_\alpha}{L}-\sum_{i=1}^{3}K_i\cdot b_i\left(-\xi_\alpha+\chi_\alpha e^{-b_iH}\right)\right)-J_{cd}=0 \quad (14)$$

In these conditions, Eq. (14) lets us obtain the junction recombination velocity's expression which depends to the illumination level n, the highest value of the short-circuit current $J_{cc\alpha}$ and the back side recombination velocity $S_{b\alpha}$.

So, the recombination velocity at the junction is expressed as follows:

$$S_{fcc\alpha}(n,J_{cc\alpha},m)=\frac{\psi(n,J_{cc\alpha}).D^{2}.\sinh\left(\frac{H}{L}\right)+M}{LD.X(m)\sum_{i}^{3}K_{i}-L\sum_{i=1}^{3}K_i.E_i(i,m)-F} \quad (15)$$

- **For a front side light:** So, we can establish the Table 2 linking some parameters of the solar cell when the latter is illuminated by its emitter. According to this table, for a front side illumination, we note that the recombination velocity to the junction as the short-circuit current grows with the light level. This result confirms once the proportionality between the charge carrier density and the light level. We also note that the short circuit current grows with the recombination velocity to the junction.
- **Recombination velocity to the junction S_{fcc2} for a back side light:** Some parameters of the solar cell are given in Table 3, for back side illumination By this Table 3 for a back side light, the analysis on the short-circuit current like on the recombination velocity to the junction remains the same as the solar cell's light by the emitter. Still, we note that these values are less important than for the front side light.
- **Recombination velocity to the junction for a simultaneous light:** The Table 4 links some parameters of the solar cell for its simultaneous light.

The interpretation of the Table 4 is identical for the front and back side illuminations. However, we note that the short-circuit current like the recombination velocities to the junction for a simultaneous illumination are more important than for the two other modes.

CONCLUSION

This study has made it possible for us to show the dependence of the photocurrent to the illumination level. No matter the number of sun, we note that the photocurrent density increases with the recombination velocity at the junction up to some value where it remains constant. Then the short-circuit condition corresponds to some S_{fcc} high values where the photocurrent tends asymptotically towards a constant value giving the short-circuit current. This situation of short-circuit corresponding to some recombination velocities very high to the junction transforms the solar cell into a current generator.

In this study we have also proposed a technic to determine the first value S_{fcc} of the recombination velocity yielding the short-circuit current and its validity domain.

REFERENCES

Alain, R., 1997. Photopiles Solaires. Presses Polytechniques et Universitaires Romandes.

Blakers, A.W., J. Zhao, A. Wang, A.M. Milne, X. Dai and M.A. Green, 1989. Proceedings of the 9th European Communities Photovoltaic Solar Energy Conference, Freiberg, September, pp: 328-329.

Bowden and A. Rohatgi, 2001. Rapid and accrute determination of series resistance and fill factor losses in industrial silicon solar celles. Proceeding of 17th European PVSEC, Munich, pp: 1802-1806.

Diallo, A., S. Maiga, A. Wereme and G. Sissoko, 2008. New approach of both junction and back surface recombination velocity in a 3D modelling study of a polycrystalline silicon solar cell. Eur. Phys. J. Appl. Phys., 42: 203-211.

Endrös, R.E. and G. Martinelli, 1997. 14th European Photovoltaic Solar Energy Conference. Barcelona, pp: 112-114.

Huljié, E.H., R. Ludemann and G. Willeke, 2001. Large area cristallin Silicon solar cells with pad printed front side metallization. Proceeding of 17th European PVSEC. Munich, pp: 1582-1585.

Mbodji, S., A.S. Maiga, M. Dieng, A. Wereme and G. Sissoko, 2010. Renoval charge technic applied to a bifacial solar cell under constant magnetic field. Global J. Pure Appl. Sci., 16(4): 469-477.

Mbodji, S., I. Ly, H.L. Diallo, M.M. Dione, O. Diasse and G. Sissoko, 2012. Modeling study of n+/p solar Cell resistances from single I-V characteristic curve considering the junction recombination velocity (Sf). Res. J. Appl. Sci., Eng. Technol., 4(1): 1-7.

Mohammad, S.N., 1987. An alternative method for the performance analysis of silicon solar cells. J. Appl. Phys. 61(2): 767.

Möller, H.J., 1993. Semiconductors for Solar Cells. Artech House, Boston, pp: 343.